Variable contact gap single-molecule conductance determination for a series of conjugated molecular bridges

2008 J. Phys.: Condens. Matter 20 374119

(http://iopscience.iop.org/0953-8984/20/37/374119)

J. Phys.: Condens. Matter **20** (2008) 374119 (9pp) doi:10.1088/0953-8984/20/37/374119

Variable contact gap single-molecule conductance determination for a series of conjugated molecular bridges

Wolfgang Haiss[1], Changsheng Wang[2], Rukkiat Jitchati[2], Iain Grace[3], Santiago Martín[1], Andrei S Batsanov[2], Simon J Higgins[1], Martin R Bryce[2], Colin J Lambert[3], Palle S Jensen[4] and Richard J Nichols[1]

[1] Centre for Nanoscale Science and Department of Chemistry, University of Liverpool, L69 7ZD, UK
[2] Department of Chemistry and Centre for Molecular and Nanoscale Electronics, University of Durham, Durham DH1 3LE, UK
[3] Department of Physics, Lancaster University, Lancaster LA1 4YB, UK
[4] Department of Chemistry, Technical University of Denmark, Kemitorvet, 2800 Kongens, Lyngby, Denmark

Received 28 March 2008
Published 26 August 2008
Online at stacks.iop.org/JPhysCM/20/374119

Abstract
It is now becoming clear that the characteristics of the whole junction are important in determining the conductance of single molecules bound between two metal contacts. This paper shows through measurements on a series of seven conjugated molecular bridges that contact separation is an important factor in determining the electrical response of the molecular junction. These data are obtained using the $I(t)$ method developed by Haiss *et al* since the scanning tunnelling microscope tip to substrate separation can be controlled through choice of the set-point (I_0) current and calibrated with current–distance curves and knowledge of the terminal to terminal length of the molecular wire. The contact gap separation dependence is interpreted as arising from tilting of these molecules in the junction and this model is underpinned by *ab initio* transport computations. In this respect we make the general observation that conductance increases rather dramatically at higher tilt angle away from the normal for conformationally rigid molecular wires and that this increase in conductance arises from increased electronic coupling between the molecular bridge and the gold contacts.

S Supplementary data are available from stacks.iop.org/JPhysCM/20/374119

(Some figures in this article are in colour only in the electronic version)

1. Introduction

Currently there is great interest in the measurement and understanding of charge transport in molecules. This has applications ranging from understanding fundamental mechanisms of charge transport in molecules to future possible uses of molecules in electronic devices. Although there have been many contributions on theoretical aspects of charge transport across individual organic molecules it has only relatively recently become possible to contact individual molecules between metal electrodes and to determine their electrical behaviour. Several approaches have been used for measuring transport through either single or small groups of molecules, including mechanically formed break junctions [1–4], break junctions formed by electromigration methods [5] and a variety of scanning probe microscopy techniques based on either STM [6–10] or conducting AFM [11, 12]. Such experiments are opening up new possibilities for understanding mechanisms of electron transport in molecules and quantifying the conductance of single molecules. In particular such measurements are helping to determine how molecular structure and electronic structure determines single-molecule conductance.

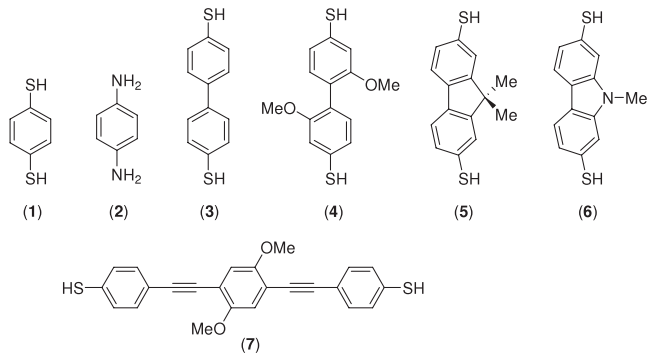

Figure 1. The compounds included in this study:
(**1**) 1,4-benzenedithiol, (**2**) 1,4-phenyldiamine,
(**3**) biphenyl-4,4′-dithiol, (**4**) 2,2′-dimethoxybiphenyl-4,4′-dithiol,
(**5**) 9,9-dimethylfluorene-2,7-dithiol,
(**6**) 9-methylcarbazole-2,7-dithiol and
(**7**) 1,4-bis[(4-mercaptophenyl)ethynyl]-2,5-dimethoxybenzene.

Recent measurements have shown that 'single-molecule conductance' (SMC) is a somewhat misleading term since the characteristics of the whole junction are important, including the contact geometry [13], the terminal groups which bind to the metal electrodes [14], the environment, the temperature [15, 16] and the tilt of the molecule in the junction [17, 18]. Understanding how the spatial separation of electrode contacts to molecules influences the electrical properties of the junction is important since nanoelectrode contacts, which may be produced in an electrical device, are likely to show a considerable spread of contact spacing. Ideally, any practical molecular electronics device would have to show tolerance to such variability; hence measuring conductance as a function of contact spacing is a significant issue in molecular electronics.

In a previous publication we have shown that the molecular conductance can be measured as a function of contact spacing controlled to sub-nanometre precision [18]. These measurements were conducted on the length-persistent molecular wire 1,4-bis[4-(acetylsulfanyl)phenylethynyl]-2,6-dimethoxybenzene (compound **7** in figure 1) and the flexible molecule nonanedithiol [18]. In this current paper we present new data that show the effect of contact gap separation on a wider range of conjugated molecular wires and show the general trend for conductance to increase rather dramatically as the contact gap is closed. The molecules selected for discussion in this paper are presented in figure 1. Compounds **1**–**7** are a series of conformationally rigid molecular wires with π-aromatic systems. SMC data determined using the $I(t)$ or the $I(s)$ method have not been previously presented for the compounds **1**–**6**. The effect of the electrode contact gap separation has been determined for these molecules and provides the core motivation for this paper. In addition, the comparison between **1** and **2** shows the influence of differing head groups. Compounds **4**, **5** and **6** on the other hand allow the influence of free rotation between the phenyl rings in **3** to be evaluated, since such free rotation is hindered for compound **4** by the methoxy substituents and is not possible at all for the conformationally fixed **5** and **6**, where the rings are locked in a coplanar alignment.

2. Experimental details

2.1. Single-molecule conductance measurements

A Pico2000 system (Molecular Imaging) STM with PicoScan 4.19 software was used throughout this study, for single-molecule conductance measurements. Details of the sample preparation and molecular adsorption on the gold films are given below. To attach molecules to the STM tip (freshly cut from a 0.25 mm gold wire (99.99%) just before each measurement), the tip is lowered onto the surface by fixing the tunnelling current I_0 at relatively high values. As described above, molecular wire formation is monitored either by the $I(t)$ or $I(s)$ techniques, whilst keeping a constant position in the x–y plane.

The key method used in this study is the $I(t)$ technique since it enables the contact gap separation to be controlled through choice of the STM set-point current. Alongside this another method has been employed for selected molecules to verify single-molecule conductance values. This is the $I(s)$ method developed by Haiss *et al*, in which tunnelling current is recorded as the molecule is stretched in a junction. The $I(s)$ and $I(t)$ methods are briefly described in the following text. For comparison, for compound **4** the break junction (BJ) method of Xu and Tao [7] has also been used.

The '$I(t)$ technique' involves holding the Au STM tip at a given distance above the substrate and then monitoring current jumps as molecular wires stochastically bridge between the tip and substrate and subsequently break. It has been previously demonstrated that $I(s)$ and $I(t)$ methods give the same G_1 for a series of alkanedithiols and viologen-containing molecular wires [10, 19]. The $I(t)$ method is the key technique in this present study since it enables control of the contact spacing through choice of the set-point current.

The $I(s)$ technique relies on contacting molecules between a gold STM tip and gold substrate and recording the current as a function of distance as the molecule is stretched until the junction is cleaved. In contrast to the case for the break junction method of Xu *et al* [7], metallic contact between the tip and surface is avoided when forming molecular junctions. $I(s)$ measurements are typically performed with a low coverage of an α, ω-dithiol molecule on a Au(111) surface. This condition enables the formation of single-molecular wires. A variety of measurements can then be performed on the analyte molecule including repeated measurement of current–distance (I–s) curves [9, 10] or the determination of current–voltage (I–V) curves for different tip–sample separations [19]. In order to attach a molecule to the STM tip, the tip is lowered onto the surface by fixing the tunnelling current I_0 at values where molecular bridges can form and then lifting it whilst keeping a constant position in the x–y plane. The current decay has been found to follow two distinctive forms. In the absence of molecular bridge formation a fast exponential decay typical of electron tunnelling between a metal STM tip and the surface is observed. On the other hand, if the molecule bridges the gap between tip and substrate a much slower decay of the tunnelling current is seen which is interrupted by a current plateau (of height I_w). As discussed previously this behaviour has been related to electron tunnelling through molecular

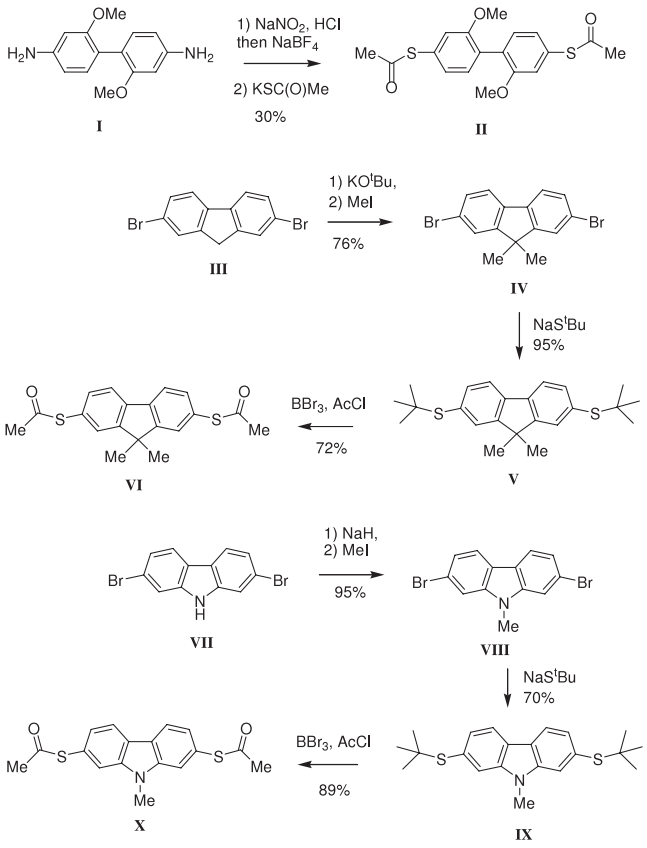

Figure 2. Synthesis procedure for compounds **II**, **VI** and **X**.

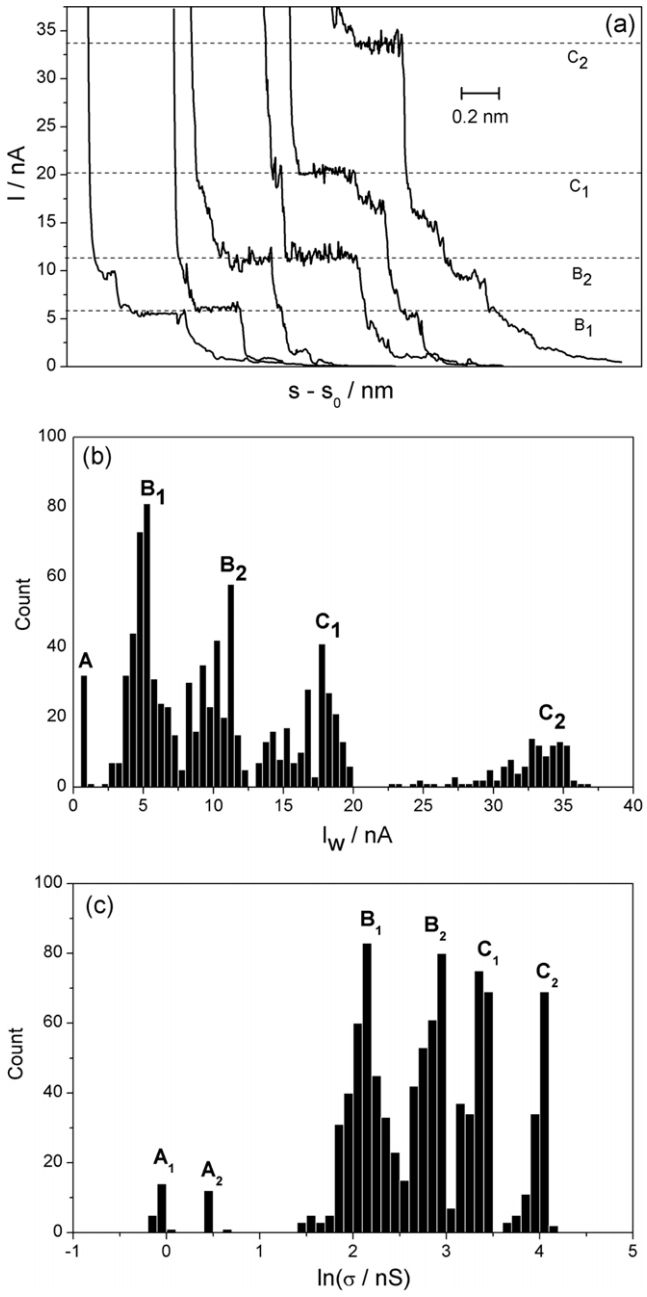

Figure 3. (a) Typical scans recorded during the tip withdrawal when molecular junctions with compound **4** are formed and then broken at bias voltage of 600 mV using the BJ method. (b) Histogram of current values constructed from 52 individual BJ scans for compound **4**. (c) A log scale conductance histogram using the data shown in (b).

wires connected between the STM tip and the substrate surface. At sufficiently large tip–sample displacements the current decreases to zero as the chemical contacts joining the molecular wires to the STM tip and the surface are broken. Statistical analysis of the data using histogram plots has shown that the current plateau values (of height I_w) group themselves at discrete values which are integer multiples of a lowest value. The lowest current peak in the histogram (I_1) is attributed to a single molecule with conductance G_1, while the next discrete conductance step at double this value (G_2) has been assigned to conduction through two wires and so on.

In the case of $I(t)$ measurements the contact gap separation is determined with a calibration of the tip–sample distance ($s - s_0$) as a function of the set-point current (I_0). This calibration is achieved by recording current–distance ($I(s)$) scans for the given sample in the absence of molecule wire formation. Typically 20 $I(s)$ scans were selected in which there were no signs of wire formation and then the slope of $\ln(I)$ versus s was determined. An average slope is then calculated within the range of I_0 values relevant to the given experiment. The z-piezo-elongation was calibrated using the height of an Au monatomic step edge (0.236 nm). A further step is then necessary to achieve an absolute separation between the STM tip and surface. In order to achieve this we used the observation that below a critical set-point current (I_c) molecular wires can no longer span the gap and hence current jumps for molecules bridging the gap are no longer observed in the $I(t)$ experiment. The assumption is that the molecule is in an upright orientation at the critical current set-point and this then provides an absolute distance calibration if the head group to head group distance for the molecule is determined using a molecular modelling program (SPARTAN®).

2.2. Materials, sample preparation and molecular adsorption

Acetyl protected derivatives of compounds **4**, **5** and **6** (namely, compounds **II**, **VI** and **X**) were synthesized in Durham following the protocols shown in figure 2. The synthetic

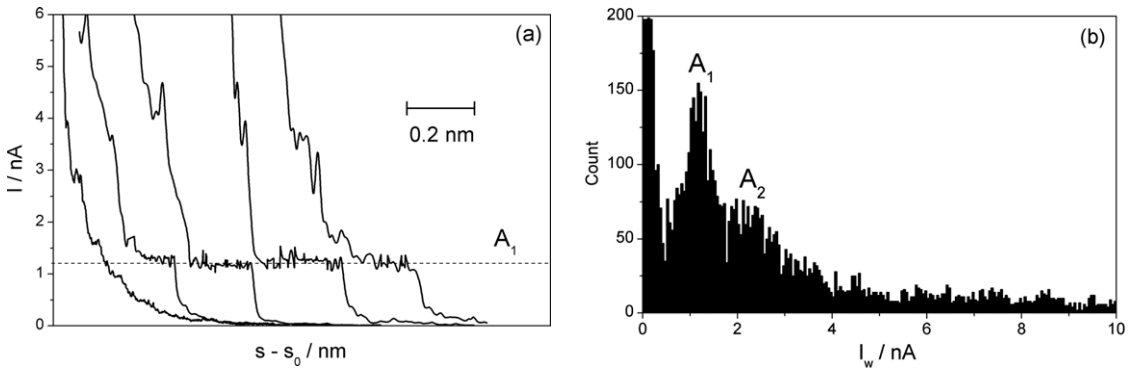

Figure 4. (a) Typical $I(s)$ example scans performed for compound **4**. For clarity the curves were stacked on the x-axis. (b) Corresponding histogram of current values constructed from 26 individual $I(s)$ curves for compound **4**. $I_0 = 10$ nA, $U_t = 600$ mV.

details and characterization data are given in the supplementary materials available at stacks.iop.org/JPhysCM/20/374119. These data include the x-ray molecular structures of compounds **VI** and **X** which showed intramolecular S . . . S distances of 10.35 and 10.27 Å, respectively. X-ray structural analysis of 2,2′-dimethoxy-4,4′-dibromobiphenyl **XI** (i.e. the dibromo analogue of **4**) showed a biphenyl twist angle of 57° in the crystal (see supplementary material figure S1 available at stacks.iop.org/JPhysCM/20/374119).

The starting point for $I(t)$ or $I(s)$ measurements is the adsorption of a low coverage of the molecular wire on a Au(111) surface. Gold films employed as substrates were purchased from Arrandee®. These were flame-annealed at approximately ∼800 °C with a Bunsen burner immediately prior to molecular adsorption. This was achieved by immersion of the flame-annealed gold films in 0.5 mM of molecule in THF for 10 s. After adsorption, the samples were thoroughly washed in ethanol and blown dry with nitrogen. These conditions are aimed at achieving low coverage of the surface which enables the formation of single-molecule wires with high probabilities in the STM experiment.

3. Experimental results

To illustrate different methods for single-molecule conductance determination we first present data recorded for compound **4** using the BJ method, the $I(s)$ and the $I(t)$ methods. Figure 3 shows typical scans recorded during the tip withdrawal, current and log scale conductance histograms for compound **4** recorded using the BJ method. Break junction experiments were realized by performing $I(s)$ scans from −2 to +3 nm at a scan rate of 50 nm s^{-1} and hence in these experiments the tip made physical contact with the surface. The tip was then retracted, resulting in the formation of a point metallic contact which is subsequently cleaved to form molecular junctions as described in the literature [7]. As the tip is further retracted these molecular junctions themselves cleave, resulting in current steps which can be represented in histogram form. Figure 3(b) shows a linear representation of the current and figure 3(c) shows a logarithmic representation of the conductance of the resulting histogram. These differing peaks have been assigned to different contact configurations of the thiol head groups and the gold contacts. In a manner similar to that of Wandlowski [20], three groups are defined, A, B and C, which are not simple multiples of each other and are attributed to differing contact configurations. On the other hand, A_2 is double the current value of A_1 and these sub-peaks (A_1/A_2, B_1/B_2 and C_1/C_2) have been attributed to one and two molecules in the junction, respectively.

Figure 4(a) shows typical $I(s)$ curves recorded for compound **4** where no contact between tip and surface was established prior to retraction ($I(s)$ method). The resulting histograms (figure 4(b)) differ from those of the BJ technique in that one group of peaks is favoured and is marked A_1 (with a shoulder marked A_2) in figure 4. Clearly the differing techniques (BJ and $I(s)$ methods) favour differing current peaks, with the BJ technique giving a higher propensity of higher current peaks (groups B and C in figure 3), while the $I(s)$ method favours the lower current **A** group of peaks. In the case of alkanedithiols these differences have been attributed to differing gold junction formations and Au–S contact configurations with the BJ technique likely to result in higher roughness following cleavage of the metallic junction. In the case of the $I(s)$ technique we found that upon increasing the step density of the gold substrate the B and C peaks increase in intensity relative to the A peaks [13]. For rough substrates the B/C peaks predominate, consistently with the notion that the BJ method favours contact to high defect density contacts.

Figure 5 shows results from the $I(t)$ method for compound **4**. Clear up and down current jumps in figure 5(a) are attributed to the stochastic attachment and detachment of thiol-linked molecular bridges between the gold tip and sample. Like for the $I(s)$ method, the low current jumps are favoured and classified as A_1 and A_2 in the histogram in figure 5(b). Such histograms have been recorded at eight different current set-point (I_0) values and the current values for the A_1 peak are plotted against the set-point current in figure 6(a). A marked dependence of the single-molecule current on the set-point current is observed. Increasing I_0 results in a decrease of the tip to sample separation (s) and as described in the methods section a distance calibration for I_0 can be obtained when the I_0 value is used together with the S–S distance for compound **4** and the 'critical current' value to provide an estimation of the contact gap separations

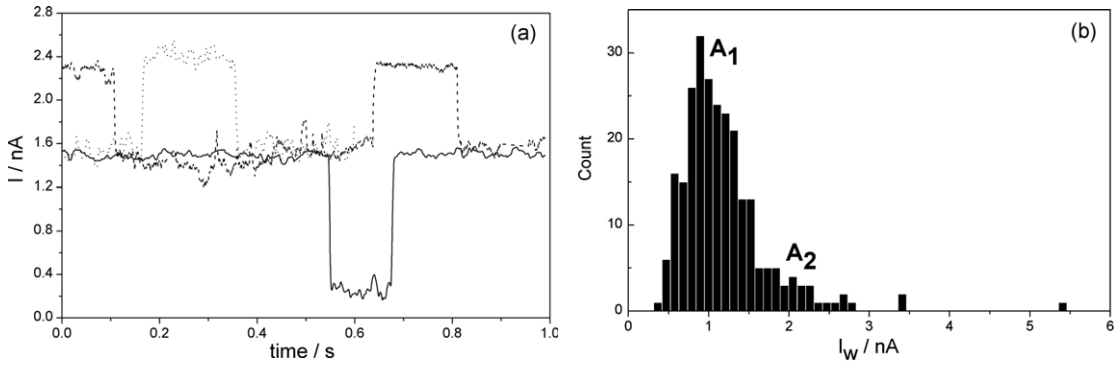

Figure 5. (a) $I(t)$ method for compound **4** showing typical current jumps. The corresponding histogram constructed from 250 jumps with $I_0 = 1.5$–5 nA and $U_t = 600$ mV is shown in (b).

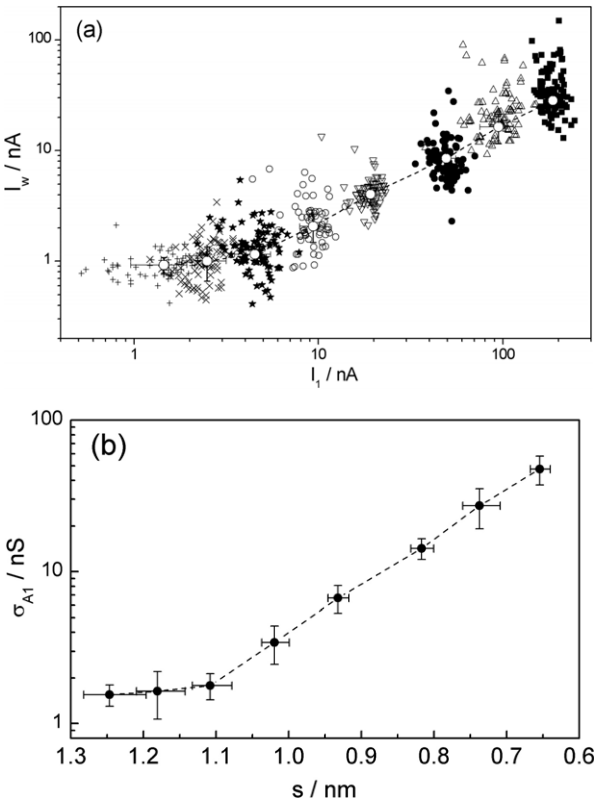

Figure 6. (a) $I(t)$ current jump values collected at different set-point currents for compound **4**. (b) SMC values as a function of tip–sample separation. Error bars: ± standard deviation.

corresponding to the selected I_0 values. With these values of contact gap separation a plot of single-molecule conductance (σ_{A_1}) versus s is obtained as shown in figure 6(b). The single-molecule conductance rises from about 1.6 nS at 1.25 nm spacing to approaching 50 nS at 0.68 nm gap spacing. Note that this latter tip to sample distance is considerably shorter than the molecular length ($d_{s-s} = 1.05$ nm) implying that the molecule must be significantly tilted in order to bridge this short gap.

Since the focus of this paper is on the contact gap separation dependence of molecular conductance we have recorded conductance histograms for compounds **1**–**6** over a range of set-point current values using the $I(t)$ technique. We then identified the A_1 current peaks from the histograms and plotted σ_{A_1} versus calibrated gap separation, as described previously. These data are collected together in figure 7.

Table 1. Single-molecule conductance values (σ_{A_1}) in the plateau region as determined by the $I(t)$ method for compounds **1**–**7**. s_{max} denotes the maximum distance between tip and sample which can be bridged by the molecule assuming upright on-top adsorption geometry and a Au–S distance of 0.25 nm. s_{onset} and θ_{onset} denote the onset of tip–sample separation and the corresponding tilt angle respectively for which a pronounced increase of σ_{A_1} was observed.

Compound	σ_{A_1} (nS)	s_{max} (nm)	s_{onset} (nm)	θ_{onset} (deg)
1	8.6	0.85	0.50	48
2	8.4	0.77	0.52	45
3	1.67	1.29	0.95	40
4	1.60	1.26	1.10	35
5	3.82	1.25	1.05	40
6	3.27	1.25	1.05	40
7	1.88	2.22	1.70	35

4. Discussion

It is clear from figure 7 that the molecular conductance shows a strong dependence on the tip to sample distance (contact gap separation). All the compounds investigated exhibit a similar behaviour characterized by a plateau region of approximately constant conductance at wider gaps which is followed by a steep rise in the current as the gap separation is decreased. In each case an onset distance (s_{onset}) can be determined, at which the current starts to rise as the gap is further closed. This onset distance is sensitive to the length of the molecule with a shorter onset distance for shorter molecules. These data are summarized in table 1 together with conductance values (σ_{A_1}) for the untilted compounds 1–7.

It is clear from table 1 that there is a strong dependence of conductance on molecular structure ranging from 1.6 nS for compound **4** to 8.6 nS for 1,4-benzenedithiol. The trends seen in the table agree qualitatively with literature values. For instance, the conductance of 1,4-benzenedithiol is higher than that of biphenyl-4,4′-dithiol which has an additional phenyl ring. Compounds **3** and **4** have comparable

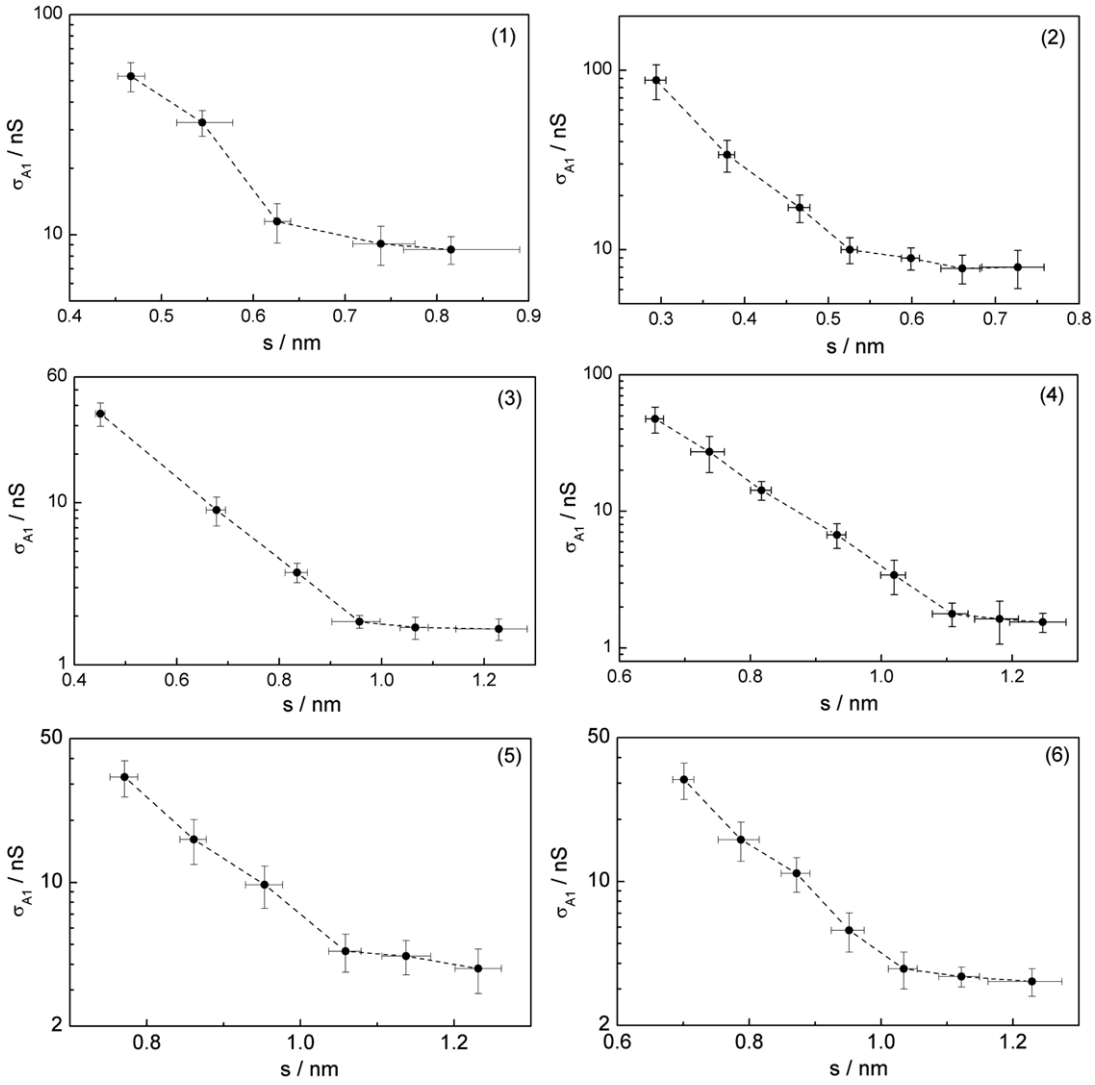

Figure 7. σ_{A_1} versus calibrated gap separation for compounds **1**–**6** as indicated by the numbers in the corresponding figures.

conductance values: notably, the additional steric effects of the methoxy substituents in **4** which would prevent coplanarity of the biphenyl system do not significantly lower the single-molecule conductance value. On the other hand, compounds **5** and **6** in which the phenyl rings are held in a coplanar configuration show a higher conductance than 4,4′-biphenyldithiol (compound **3**) which allows free rotation about the C–C bond. This is in agreement with previous measurements by Venkataraman *et al* [21] which have established this link for a series of molecules exhibiting various twist angles between adjacent rings.

All of the compounds studied here show a strong dependence of the molecular conductance on the contact gap separation as the gap is closed beyond a certain separation which is marked in the table as s_{onset}. This value of s_{onset} increases with molecular length implying that molecular tilt is an influential factor for molecular conductance value. This assertion is corroborated by the rather similar values of the onset of the strong tilt angle dependence (θ_{onset}), which is in the range of 35°–50° for all compounds studied. The tilt angle dependence has been previously rationalized with a detailed theoretical investigation of electron transport through 1,4-bis[4-(acetylsulfanyl)phenylethynyl]-2,6-dimethoxybenzene attached between gold contacts [18]. These computations showed that as the tilt angle increases the HOMO and LUMO resonances broaden and shift to lower energies. This indicated that the strength of the coupling between the gold contacts and the molecule increases with increasing tilt angle and that this is the underlying physical reason behind the increase in conductance with tilt angle. The current observations experimentally confirm this phenomenon for a number of other molecules with thiol anchoring groups and compound **2** with different anchoring groups (–NH_2).

Data for 1,4-benzenedithiol (**1**) and biphenyl-4,4′-dithiol (**3**) are compared in figure 8. The two molecules exhibit a similar behaviour upon tilting, with a rather invariant region up to ∼40°–50° tilt, followed by a sharp tilting dependence at >40°–50°. A β_N value of 1.64 is estimated for the plateau region, consistent with experimental [22, 23] and theoretical [24, 25] literature values. The biphenyl-4,4′-dithiol system adds the extra complexity of free rotation about the C–C bond which interconnects the two phenyl rings.

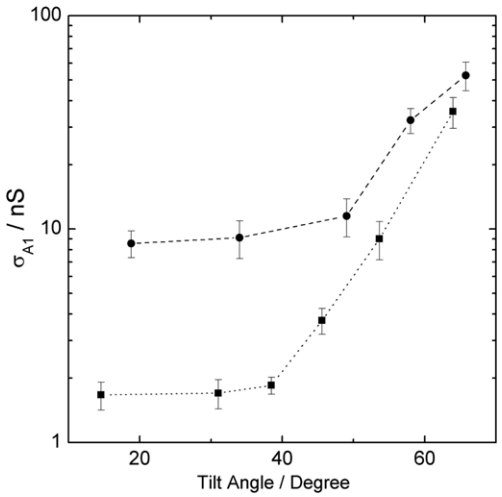

Figure 8. Comparison of angle dependences for 1,4-benzenedithiol (compound **1**; circles) and biphenyl-4,4′dithiol (compound **3**; squares). A beta value of 1.64 per phenyl group results from the conductance ratio at small tilt angles, consistent with literature values.

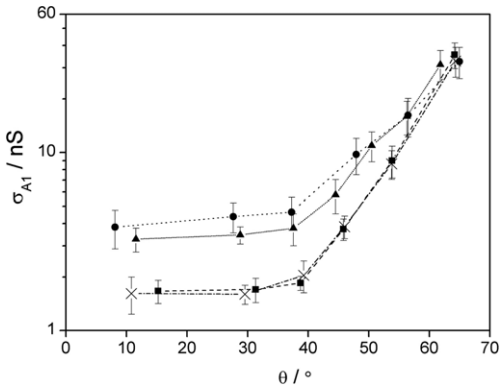

Figure 9. A_1 SMC versus tilt angle (θ) for compound **3** at 20 °C (squares) and 80 °C (crosses) and compound **6** (triangles) and compound **5** (circles).

As the 1,4-benzenedithiol molecular bridge is tilted in the junction it seems likely that free rotation around this C–C bond will be impeded due to spatial confinement. In order to accommodate this confinement the phenyl rings are likely to be forced into a more coplanar and correspondingly more conductive configuration (see the discussion in section 5). This additional complexity of ring rotation does not occur for compounds **5** and **6**, since in these compounds the two rings are rigidly held in a coplanar conformation. Data for these two compounds are shown together with data for 4,4′-biphenyldithiol in figure 9. For all three compounds at small tilt angles ranging from about 0° to 40°, corresponding to wider contact gaps, the conductance is rather invariant. However, at larger tilt angle the conductance increases dramatically. Figure 9 also presents data for biphenyl-4,4′-dithiol at two temperatures showing that there is no dependence of the conductance on temperature between 20 and 80 °C, consistently with the notion that temperature dependence in not seen in this range for conformationally rigid molecules [18].

5. Theory

We now investigate the theoretical tilt dependence for the thiol terminated compounds **1**, **3**, **5** and **6**. Compound **7** has been studied previously [18]. For each molecule the following method was applied. To begin with, the relaxed geometry of the molecule was found using the density functional (DFT) code SIESTA [26]. The molecule was then extended, by including six layers of the gold leads on the top and bottom surfaces. Each layer of the Au(111) slab comprised 25 atoms and was chosen to provide a large enough surface area to include the effects of creating a large tilt angle. Six layers of gold are sufficient to allow a suitable representation of charge transfer effects at a molecule–gold interface. Using the recently developed, '*ab initio*', non-equilibrium Green's function, SMEAGOL method [27], to calculate the electron transport coefficients for each tilt angle we define the orientation of the molecule between the leads by two angles (figure 10(a)): θ which defines the tilt angle of the molecule away from the normal and ϕ which is the angle of rotation of the whole molecule about its axis.

Compounds **5** and **6**, as described previously, are coplanar while 4,4′-biphenyldithiol (compound **3**) has a ring twist. The optimum geometry calculated using DFT finds this torsion angle to be approximately 38°. The experimental data show that the conductance of compound **3** is approximately a factor of 2 smaller than that for the planar molecule; this is in agreement with the expected $\cos^2$ dependence of the twist angle [21, 28]. To model this we first calculated the coefficients for zero-bias transmission through compounds **3** and **5** for a tilt angle of $\theta = 0°$; the dependence on ϕ in this case is negligible. Figure 10(b) shows the typical resonant behaviour for the two molecules with the Fermi energy (0 eV) lying in the gap between the HOMO and LUMO resonances. Comparing the conductance at the Fermi energy for the planar compound **5** (solid line), $G(E_F) = (6.9 \times 10^{-4})G_0$, with that for the twisted compound **3** (dotted line), $G(E_F) = (4.1 \times 10^{-4})G_0$, we see the expected reduction in the conductance. Therefore, in the non-tilted case the theoretical behaviour follows the expected $\cos^2$ for the twisting of the rings.

We now examine how the conductances of compounds **3** and **5** alter as the value of θ is increased from 0° to 70°. This calculation is produced in two parts. Firstly the optimum value of ϕ for each value of θ is found using DFT. Here we define an angle $\phi = 0°$ to correspond to the case where the end phenyl ring is oriented perpendicular to the bottom gold surface and an angle $\phi = 90°$ then applies to the case where the phenyl is oriented parallel to the bottom surface. Using this optimum orientation, the conductance is then calculated at the Fermi energy. Figure 11(a) shows the computed conductances for compound **3** (squares) and compound **5** (circles). The conductances for the two molecules follow the same general behaviour with only a difference in magnitude due to the non-coplanarity of the phenyl rings of compound **3**. At low tilt angles the conductance remains constant and then for

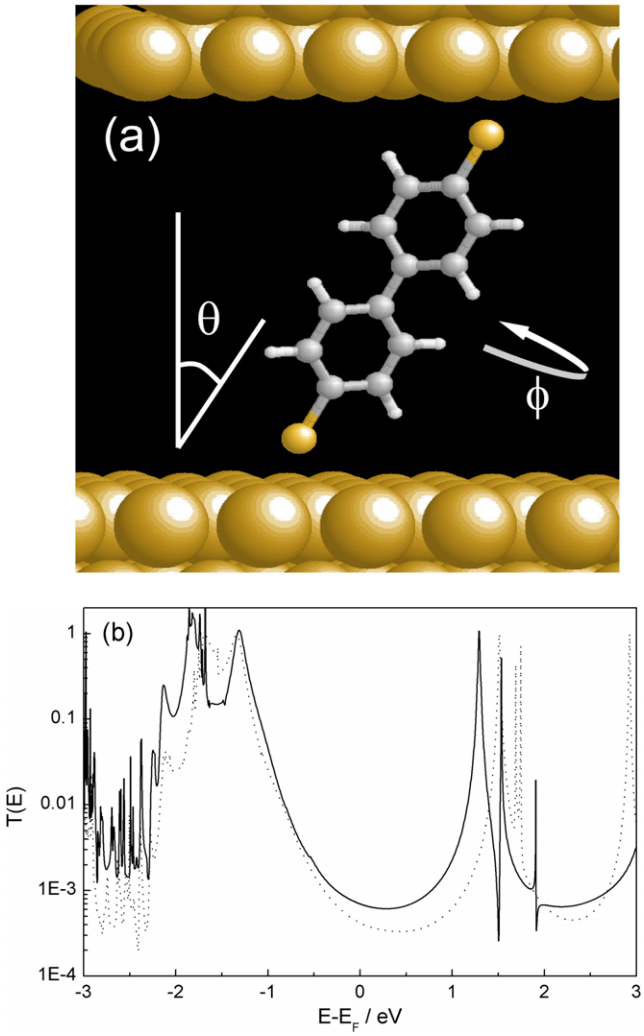

Figure 10. Orientation of molecule **3** between Au(111) contacts (a). Zero-bias transmission coefficient for compound **3** (dotted line) and compound **5** (solid line) for $\theta = 0$ and $\phi = 0$.

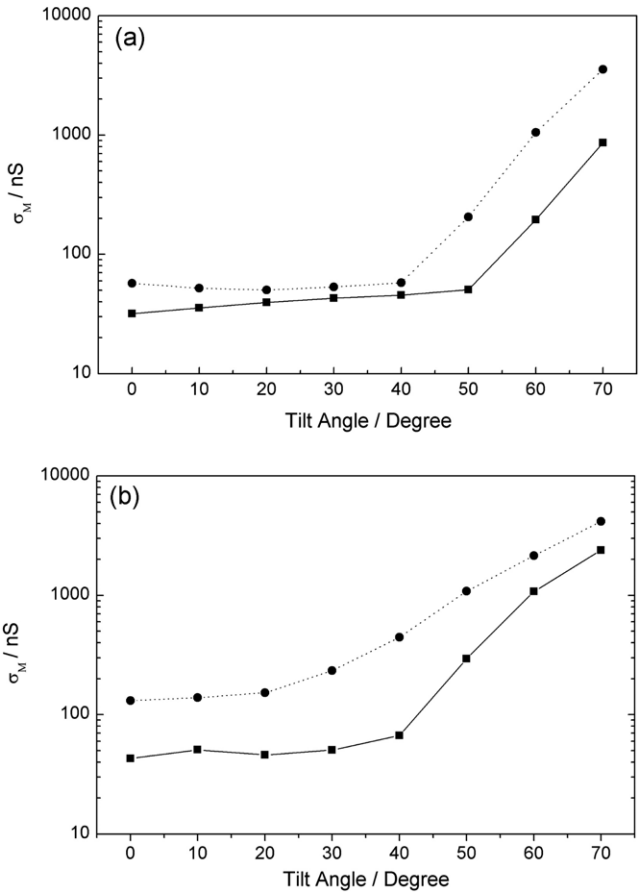

Figure 11. (a) Conductance against tilt angle for compound **3** (squares) and compound **5** (circles). (b) Conductance against tilt angle for compound **1** (circles) and compound **6** (squares).

angles greater than 50° begins to increase. This behaviour can be explained by a change in the value of ϕ, which for low values of θ is approximately 0°, but at angles beyond 50° it increases due to interactions between the end phenyl rings and the gold surfaces. Previous work on compound **7** has shown that increasing the value of ϕ significantly increases the conductance at the Fermi energy and this was explained by an increase in the strength of the coupling which broadens the resonances [18]. These computational results show good qualitative agreement with the experimental data of figure 9, but the computed magnitude of the conductance is approximately one order of magnitude greater.

Compound **6** differs from **5** only in the structure of the bridge which coplanarizes the two rings. Figure 11(b) (squares) shows the tilt dependence for compound **6** which again demonstrates the same behaviour as figure 11(a). Comparing compounds **5** and **6** reveals that the magnitudes are very similar and suggests that the side group has little effect on the conductance through these molecules. This is again in good agreement with the experimental findings. Lastly we look at the length dependence. Compound **1** only consists of one ring and its tilt dependence is shown in figure 11(b) (circles). Here the conductance again displays the same tilt angle dependence, where the conductance of the untilted molecule is approximately a factor 3–4 larger than those for compounds **3**, **5** and **6**.

This theoretical model offers a simple picture for describing the behaviour seen in the experimental measurements; the increase in conductance results from changes in the strength of coupling between the molecule and the gold surfaces as the molecule is tilted. The steep increase of conductance beyond tilt angles of 40° occurs because of a change in the orientation of the molecule which alters the value of ϕ.

Acknowledgments

This work was supported by EPSRC under grant EP/C00678X/l (Mechanisms of Single Molecule Conductance) (Liverpool) and Basic Technology grant GR/S84064/01 (Controlled Electron Transport) (Durham). RJ thanks the Royal Thai Government for the award of a scholarship. SM acknowledges a postdoctoral fellowship from Ministerio de Educacion y Ciencia of Spain.

References

[1] Reed M A, Zhou C, Muller C J, Burgin T P and Tour J M 1997 *Science* **278** 252
[2] Kergueris C, Bourgoin J P, Palacin S, Esteve D, Urbina C, Magoga M and Joachim C 1999 *Phys. Rev.* B **59** 12505
[3] Weber H B, Reichert J, Ochs R, Beckmann D, Mayor M and von Lohneysen H 2003 *Physica* E **18** 231
[4] Reichert J, Ochs R, Beckmann D, Weber H B, Mayor M and von Lohneysen H 2002 *Phys. Rev. Lett.* **88** 176804
[5] Park H, Lim A K L, Alivisatos A P, Park J and McEuen P L 1999 *Appl. Phys. Lett.* **75** 301
[6] Yazdani A, Eigler D M and Lang N D 1996 *Science* **272** 1921
[7] Xu B Q and Tao N J J 2003 *Science* **301** 1221
[8] Dorogi M, Gomez J, Osifchin R, Andres R P and Reifenberger R 1995 *Phys. Rev.* B **52** 9071
[9] Haiss W, van Zalinge H, Higgins S J, Bethell D, Hobenreich H, Schiffrin D J and Nichols R J 2003 *J. Am. Chem. Soc.* **125** 15294
[10] Haiss W, Nichols R J, van Zalinge H, Higgins S J, Bethell D and Schiffrin D J 2004 *Phys. Chem. Chem. Phys.* **6** 4330
[11] Cui X D, Primak A, Zarate X, Tomfohr J, Sankey O F, Moore A L, Moore T A, Gust D, Harris G and Lindsay S M 2001 *Science* **294** 571
[12] Leatherman G, Durantini E N, Gust D, Moore T A, Moore A L, Stone S, Zhou Z, Rez P, Liu Y Z and Lindsay S M 1999 *J. Phys. Chem.* B **103** 4006
[13] Haiss W, Martín S, Leary E, van Zalinge H, Higgins S J and Nichols R J 2008 in preparation
[14] Chen F, Li X L, Hihath J, Huang Z F and Tao N J 2006 *J. Am. Chem. Soc.* **128** 15874
[15] Haiss W, van Zalinge H, Bethell D, Ulstrup J, Schiffrin D J and Nichols R J 2006 *Faraday Discuss.* **131** 253
[16] Jones D R and Troisi A 2007 *J. Phys. Chem.* C **111** 14567
[17] Kornilovitch P E and Bratkovsky A M 2001 *Phys. Rev.* B **64** 195413
[18] Haiss W, Wang C S, Grace I, Batsanov A S, Schiffrin D J, Higgins S J, Bryce M R, Lambert C J and Nichols R J 2006 *Nat. Mater.* **5** 995
[19] Haiss W, van Zalinge H, Hobenreich H, Bethell D, Schiffrin D J, Higgins S J and Nichols R J 2004 *Langmuir* **20** 7694
[20] Li C, Pobelov I, Wandlowski T, Bagrets A, Arnold A and Evers F 2008 *J. Am. Chem. Soc.* **130** 318
[21] Venkataraman L, Klare J E, Nuckolls C, Hybertsen M S and Steigerwald M L 2006 *Nature* **442** 904
[22] Wold D J, Haag R, Rampi M A and Frisbie C D 2002 *J. Phys. Chem.* B **106** 2813
[23] Wakamatsu S, Fujii S, Akiba U and Fujihira M 2003 *Ultramicroscopy* **97** 19
[24] Sun Q, Selloni A and Scoles G 2006 *J. Phys. Chem.* B **110** 3493
[25] Cohen R, Stokbro K, Martin J M L and Ratner M A 2007 *J. Phys. Chem.* C **111** 14893
[26] Soler J M, Artacho E, Gale J D, Garcia A, Junquera J, Ordejon P and Sanchez-Portal D 2002 *J. Phys.: Condens. Matter* **14** 2745
[27] Rocha A R, Garcia-Suarez V M, Bailey S, Lambert C, Ferrer J and Sanvito S 2006 *Phys. Rev.* B **73** 085414
[28] Woitellier S, Launay J P and Joachim C 1989 *Chem. Phys.* **131** 481